Yielding behavior and temperature-induced on-field oscillatory rheological studies in a novel MR suspension containing polymer-capped Fe_3Ni alloy microspheres

Injamamul Arief[a,*], P.K. Mukhopadhyay[b]

[a] Department of Materials Engineering, Indian Institute of Science, Bangalore 560012, India
[b] LCMP, Department of Condensed Matter Physics and Material Sciences, S. N. Bose National Centre for Basic Sciences, Salt Lake, Kolkata 700 106, India

Keywords:
PAA-Fe_3Ni microspheres
Yield stress
Multipolar interaction
Temperature-dependence
Oscillatory rheology
Complex moduli

A B S T R A C T

Magnetic Bimetallic alloy nanoparticles of 3d elements are known for their tunable shape, size and magnetic anisotropy and find extensive applications ranging from magneto-mechanical to biomedical devices. This paper reports the polyol-mediated synthesis of Fe-rich polyacrylic acid (PAA)-Fe_3Ni alloyed microspheres and its morphological and structural characterizations with scanning electron microscopy and X-ray diffraction studies. Magnetorheological fluid was prepared by dispersing the 10 vol% microparticles in silicone oil. The room temperature viscoelastic characterization of the fluid was performed under different magnetic fields. The field-dependent yield stresses were scaled using Klingenberg model and found that static yield stress was more accurately described by an ~M^3 dependence, where M is particle magnetization. We proposed a multipolar contribution and ascertained the fact that simple dipolar description was insufficient to describe the trend in a complex rheological fluid. Temperature-dependent oscillatory rheological studies under various fields were also investigated. This demonstrated a strong temperature-induced thinning effect. The temperature-thinning in complex moduli and viscosity were more pronounced for the samples at higher magnetic field owing to quasi-solid behavior.

1. Introduction

Ferromagnetic nanomaterials are the subject of immense interest since last couple of decades due to certain properties that make them suitable in smart devices, biomedical and technological applications [1–3]. Magnetic saturation of these ferromagnetic nano and micro-structures is dependent on the shape, size and composition. The tunable magnetic properties of functional nano and microstructures have been the subject of interests and studied extensively. For specific applications such as magnetic fluids and magnetorheological clutches and dampers, a high stress output is required [4–6]. The strength of field-induced structural aggregates is a direct function of magnetic saturation [4,7]. Therefore the goal in fabrication of magnetic particles is to have higher magnetic saturation and lower coercivity and remanence. In contrast to conventional carbonyl iron particles (CIP), ferromagnetic binary alloys of *3d* transition metals proved to be excellent materials for magnetorheological application and have been studied previously [8,9]. In addition to FeCo and NiCo, FeNi alloys are of great interest due to wide ranges of useful magnetic and mechanical properties [9]. Notably, FeNi is a soft magnetic material with high saturation magnetization, low coercivity [9], high magnetic permeability, low thermal expansion [10], and excellent corrosion resistance [11]. It was shown before that for both bulk and nano-size, magnetic properties for FeNi alloys with a specific composition are a function of different combination of *bcc* and *fcc* phases. In practice, when two phases coexist, the relative amount/percentage so obtained appears also to depend on the preparation method [12].

To improve the applicability of FeNi alloyed microparticles in MR fluidic applications, it is necessary to modify and functionalize surfaces of particles so as to increase the soft magnetic properties for custom MR application. These structures are classified as composites microstructures. Composite materials offer distinct multifunctional properties which could be optimized for desired applications. Metal alloy-polymer composites exhibit excellent physical, chemical, and mechanical properties that single phase materials do not possess. Furthermore, striking feature of bimetallic materials over their single metal analogues (Fe, Co, or Ni) lies in their tunable magnetic and morphological behavior. By careful control of the precursor concentrations and capping agents in bottom up chemical approaches, one can effectively modify the shape, size, magnetization and surface properties.

* Corresponding author.
E-mail address: arif.inji.chem1986@gmail.com (I. Arief).

In this paper, we report the fabrication and characterization of polyacrylic acid (PAA)-capped Fe_3Ni-based magnetorheological (MR) fluids which has not been studied so far. While Fe-rich alloy systems with considerably high saturation magnetization enhance MR effect significantly, PAA-encapsulation offers higher sedimentation stability as well as chemical stabilization from oxidation. By encapsulation of PAA, interparticle adhesion can be greatly controlled whereas, the hierarchical shape of microparticles can be reproduced by the capping action of electron-rich PAA. Steady shear magnetorheological studies revealed desired MR response under increasing magnetic field. The field-induced stress relaxation measurements provided useful insight into on-field structuration and subsequent relaxation upon removal of field. The material performance of MR fluid can be greatly compromised at higher temperature. The increased operating temperature can also affect the applications in engineering. An MR device dissipates energy in the form of heat and therefore, increases the device temperature [13]. So, operability of MR fluids at elevated temperature is fundamental to MR studies and therefore, to be thoroughly addressed in order to predict the effect of temperature on the MR effect and the mechanisms that influence the fluid behavior. We have investigated the temperature dependent oscillatory magnetorheology with 10 vol% MR fluid containing PAA-Fe_3Ni in a typical, high viscosity carrier liquid. Temperature-induced thinning effect in MR properties is evident for the samples under investigation.

2. Experimental details

Hydrazine reduction of Fe (II) chloride (Merck) and Ni (II) acetate in 1:1 water-ethanol precursor solution is described as follows: Ni (II) acetate, Fe (II) chloride and poly-acrylic acid (PAA, avg. mol. wt. ~1800, Sigma-Aldrich) were dissolved in 30 mL 1:1 water-ethanol solution ($[Ni^{2+}]$ =0.02 M, $[Fe^{2+}]$ =0.06 M, [PAA] =0.1 M). Separately, sodium hydroxide (NaOH) and hydrazine hydrate (0.2 M, Ranbaxy) were dissolved in water-ethanol solution. The two solutions were mixed together under continuous and vigorous stirring in a magnetic stirrer. The temperature was raised to 65 °C under constant purging of Argon (Ar) gas into the solution. The reaction was continued for 2 h. Afterwards, the resultant product was washed thoroughly with deionized water for removal of reaction residues followed by washing with acetone. Finally, the black particles were soaked in ethanol in a closed container for further characterization. The PAA was involved in surface functionalization and structural evolution of Fe_3Ni nanospheres. Final shape of the nanoparticles was evolved through LaMer's method of fast super-saturated burst nucleation mechanism followed by aggregation and subsequent growth to microspheres [14]. The MR fluid was prepared by dispersing 10 vol% Fe_3Ni into castor oil (viscosity 0.879 Pa s at 25 °C) through mechanical stirring and ultrasonication. The density of as-synthesized Fe_3Ni particles was found out to be 6.2 g/cm^3.

Particle morphology, size and shape were investigated by a field emission scanning electron microscope (Quanta FEG, FEI). Crystal structures and phases of the powdered samples at room temperature were investigated by powder x-ray diffraction using a PANalytical X′Pert PRO® diffractometer using monochromatic Cu-Kα radiation (λ=0.51418 nm). Room temperature magnetometric study of sample pellets (pressed powder) was performed on a Lakeshore Cryotonics® Inc. model 7400 VSM. Field-dependent magnetorheological measurements were performed using a commercial rheometer (Anton Paar MCR Physica 501) with magnetorheological attachment (MRD 170®) in strain controlled mode. The parallel plate system with plate diameters of 20 mm was used for all measurements. A fixed plate-gap of 1 mm was maintained throughout the measurements. Prior to any measurement, the sample was pre-sheared at 20 s^{-1} for about 30 s. In steady shear experiment, field was varied from 0.1 to 0.5 T. The

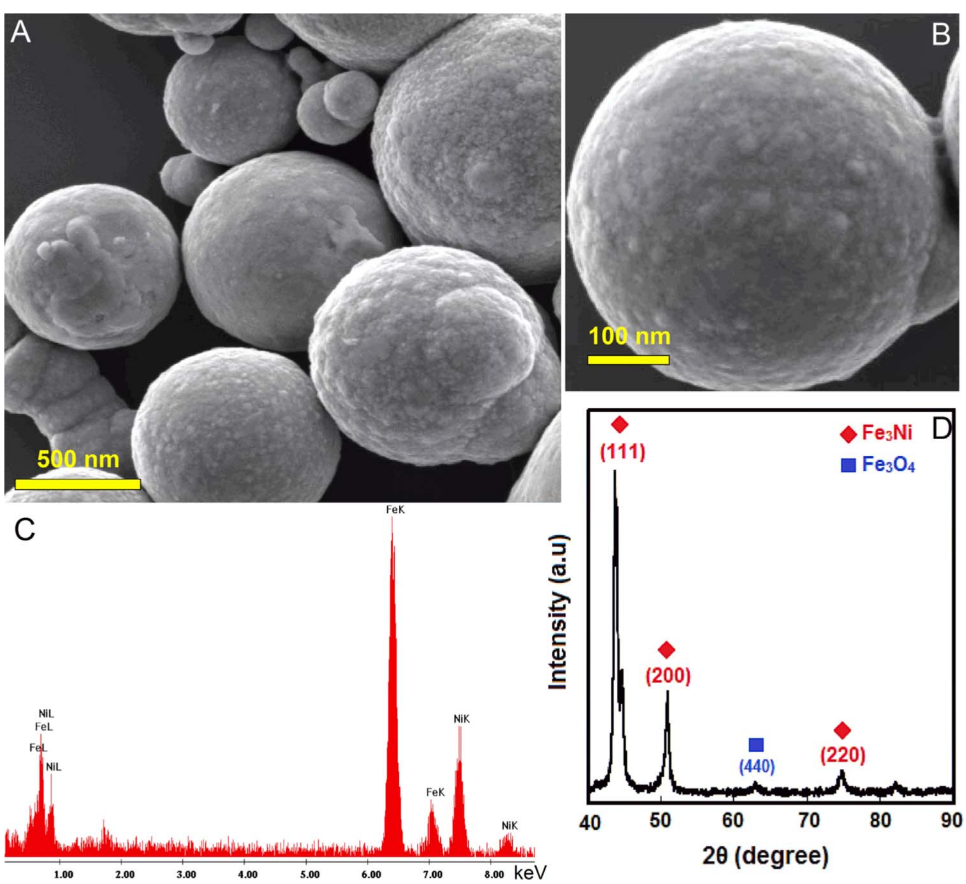

Fig. 1. (A, B) Low and high magnification FESEM images of PAA-Fe_3Ni, (C) EDAX spectra and (D) X-ray diffraction patterns of Fe_3Ni microspheres.

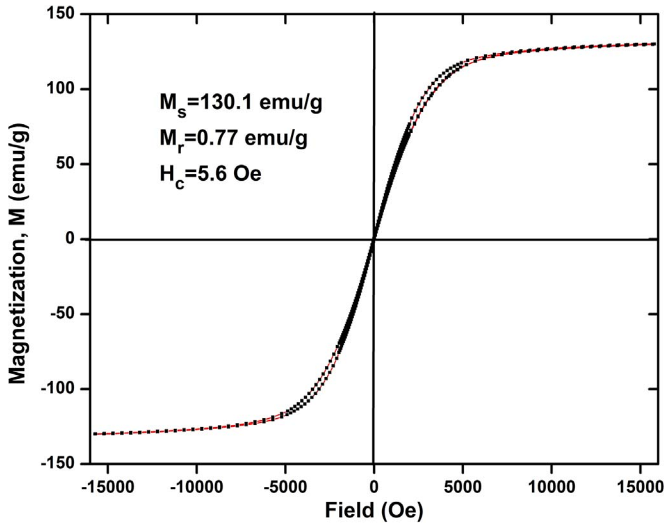

Fig. 2. Room temperature M-H hysteresis curve of PAA-Fe_3Ni sample.

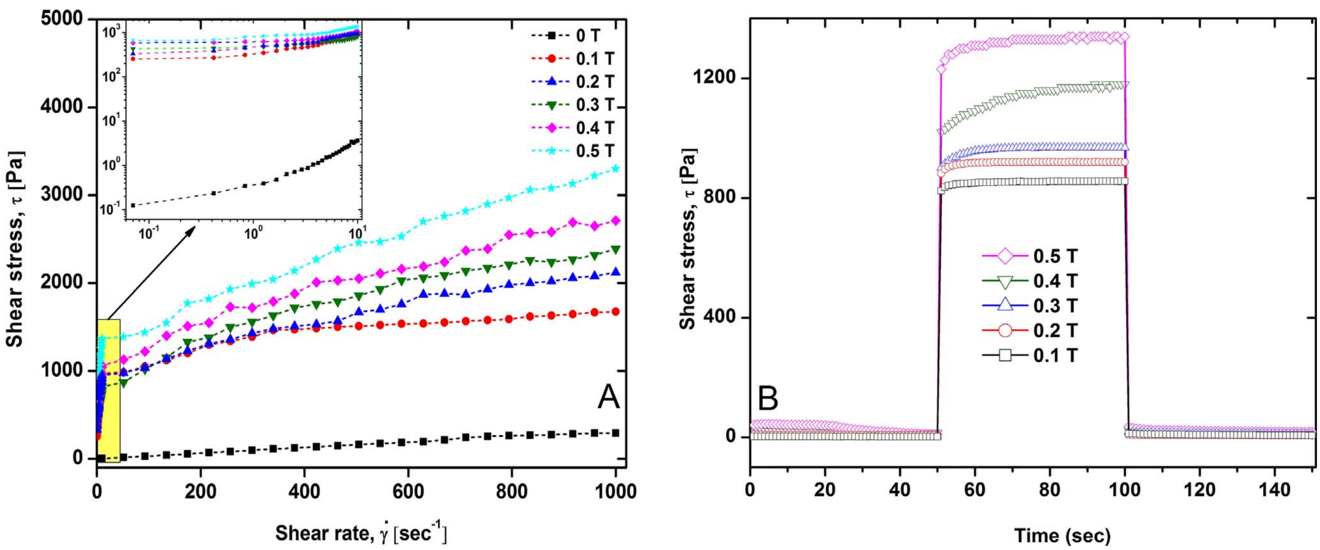

Fig. 3. (A) Steady shear rheological behavior of MR fluids for different magnetic fields. (B) Field-induced shear stress relaxation with time.

temperature sweep oscillatory measurements were performed under constant amplitude strain of 0.02% and frequency 10 Hz. The temperature was varied from 19 °C to 55 °C. The results were recorded under different magnitude of magnetic field, ranging from 0.1 to 0.5 T.

3. Results and discussions

3.1. Structure and morphology

The morphology, composition and crystal structures of as-prepared Fe_3Ni are investigated using FESEM (FEI Quanta FEG), EDAX and XRD (Panalytical XpertPro). The low and high magnification FESEM images of Fe_3Ni are shown in Figs. 1A and B. Images show well-dispersed spherical Fe_3Ni-nanocomposite particles prepared using PAA polymer. Sub-micron sized Fe_3Ni microparticles are secondary particles formed by nucleation and subsequent growth of primary nanoparticles thus formed. The surfaceof microspheres appeared to be rough, owing to polymer encapsulation during the growth phase. The average (mean) diameter of Fe_3Ni is found to be 700 nm. The composition of alloyed microstructures are determined by EDAX analysis and shown in Fig. 1C. It confirms the final composition of Fe_3Ni is consistent with the initial molar concentrations of metal salts. The material is, therefore, nearly uniform Fe_3Ni solid solution of Ni in Fe with very little deviation in composition for different sized particles. The composition of crystal phase of as-synthesized Fe_3Ni powder is characterized by XRD, and the XRD patterns of sample is shown in Fig. 1D. Three characteristic peaks for *fcc* Fe_3Ni (2θ=44.1°, 51.5°, 76.1°), correspond to Miller indices (111), (200), (220) are observed. However, in addition to Fe_3Ni, peak corresponds to Fe_3O_4 can also be detected, as unreacted Fe may form oxides during the reaction. This indicates that Fe^{2+} was not reduced into Fe completely. The average size of the crystalline domains (coherently diffracting domains) of the sample is calculated from the broadening of the (111) X-ray diffraction peak using the Scherrer equation [15]: $\beta_{hkl} = k.\lambda/L_{hkl}.\cos\theta$, where β_{hkl} is the broadening of the diffraction line measured at full width half maximum intensity (FWHM), $\boldsymbol{\lambda}$ is the X-ray wavelength, L_{hkl} is the crystal size and θ is the diffraction angle, k is the Scherrer shape factor (k=0.9 for the calculations). The calculated average crystallite size for the as-prepared Fe_3Ni is 38 ± 5 nm. The room temperature magnetization studies (Fig. 2) in vibrating sample magnetometry (M-H hysteresis curve) show that the material is magnetically soft with low coercivity (H_c) and remanence (M_r) whereas, saturation magnetization (M_s) is quite high. The H_c, M_r and M_s of PAA-Fe_3Ni are measured to be 5.62 Oe, 0.77 emu/g and 130.1 emu/g, respectively.

3.2. Magnetorheological studies

3.2.1. Steady shear magnetorheology in PAA-Fe_3Ni based MR fluid

Rheological measurements were carried out under different magnetic fields, ranging from 0 to 0.5 T under steady shear mode and are shown in Fig. 3. Shear stresses are plotted as a function of shear rate for MRF containing 10 vol% of PAA-Fe_3Ni microspheres under different magnetic flux as shown in Fig. 3A. The rheograms illustrate the desired magnetorheological behavior with shear stress increasing predictably and systematically with shear rate. The rheograms show a typical Bingham plastic behavior, characterized by field-dependent (dynamic) yield stress. Dynamic or Bingham yield stress is calculated according to Bingham equation,

$$\tau = \tau_{ys} + \eta\dot{\gamma},$$

where τ, τ_{ys}, η and $\dot{\gamma}$represent shear stress, dynamic yield stress, viscosity and shear rate, respectively [16]. The data points in the measurements are divided into two different shear rate windows, at low shear rate (0.001–10 s^{-1}) and in the high shear regime, typing in the range of 10–1000 s^{-1}.

These two shear regimes account for two types of yield stresses,

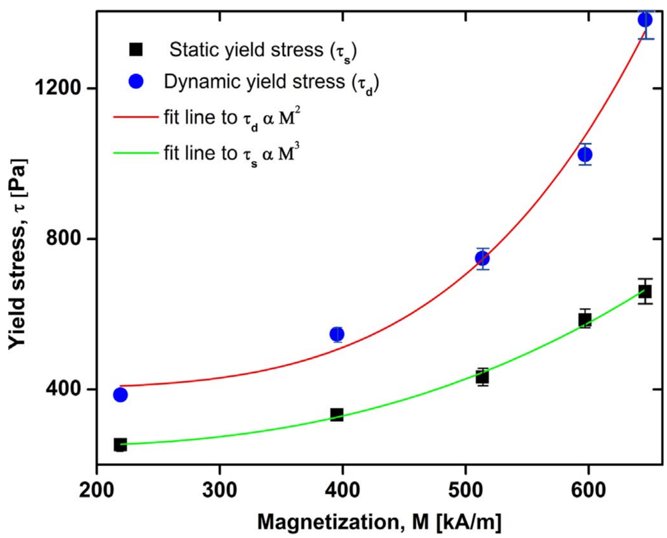

Fig. 4. Field-induced static (square) and dynamic (circle) yield stress for MR fluid as a function of particle magnetization M.

namely static and dynamic yield stress. The zoomed in section of rheogram in the 0.05–10 s^{-1} is shown in the inset of Fig. 3A. The static yield stress is defined as the threshold or initial shear point at very low shear rate that indicates the commencement of fluid flow. The dynamic or Bingham yield stress can be estimated from Bingham equation fitting as shown above. Therefore, this is the extrapolated value at which the plastic flow would have occurred first. Since this is the major portion in the strain–strain rate curve in which the intended device will operate, it is also a very important parameter. In absence of field, MRF possesses non-zero yield stress under low shear rate and it increases with increasing magnitude of the applied field. As polymer (PAA)-assisted growth of microspheres introduces surface roughness, strong chain-like microstructures are formed due to intense particle-particle interaction under shear. Increasing magnetic field strength also facilitates stronger interaction, thus giving rise to higher field-dependent yield stress. In presence of magnetic field, shear stress dramatically increases with magnetic field as higher yield stresses are shown for the MR fluid. In Fig. 4, static and dynamic yield stresses of the MRF are shown as a function of particlemagnetization extracted from powder magnetization data [17]. According to Klingenberg et al., a better correlation of yield stresses is observed when external magnetic field is replaced by particle magnetization [18]. As was the case with NiCo-

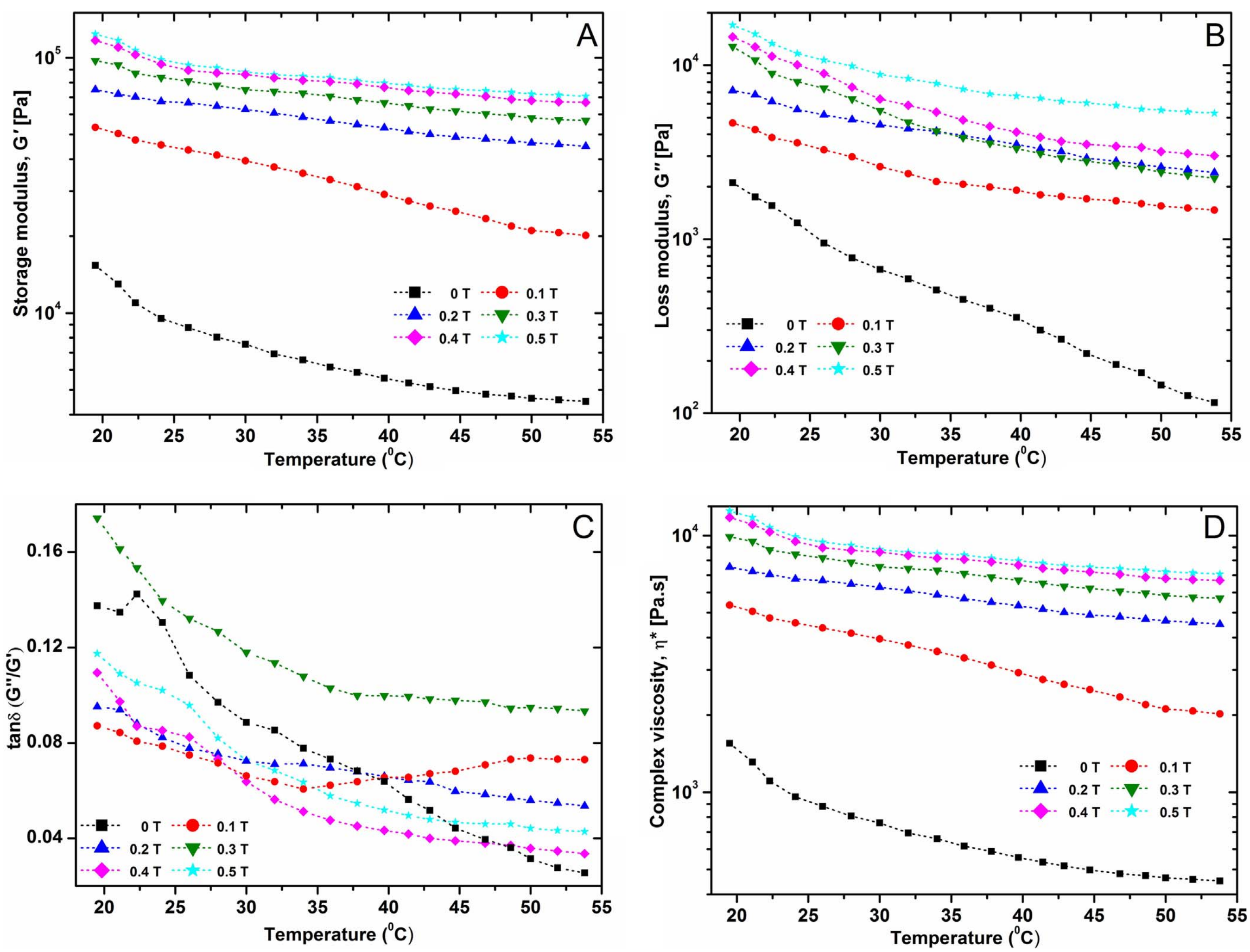

Fig. 5. Storage (G′) and loss moduli (G′′) as a function of temperature and magnetic fields (A, B); loss factor versus temperature (C) and complex viscosity as a function of temperature (D) are shown.

based systems, which has been reported in our earlier work, Ginder's law was insufficient to contain all the data points in sub-quadratic scaling of yield stresses as given below:

τ_{ys}=2. 45$\phi\mu_0 M_s^{1/2} H^{3/2}$,

$\phi HkA/mM_s$[19,20]$_{\text{yd}}{}^{232}$[18][19]$^2\mu_0 4\pi\times10^{-7}$H/m

Shear stress relaxation with time as a function of magnetic field is shown in Fig. 3B. The field-induced relaxation of stress is observed at room temperatures and at CSR mode under constant shear rate (10 s^{-1}). The timescale was divided into three timescale zones; in the first and third zones, field is set to be zero whereas in intermediate zone, magnetic fields in the range 0.1–0.5 T are applied. Time delays for data acquiring was 1 s for all the data points. An obvious trend in field-induced stress is observed in the on-field region as with high field, strongly aggregated particle networks yield higher stress. As soon as the field is switched on, an instantaneous jump in shear stress is shown owing to field-induced aggregation of microspheres. Since the timescale of data acquisition is much faster than the structural relaxation (relaxation time), we observe an immediate fall after the field is switched off. The characteristic relaxation time increases with increasing magnetic field. This phenomenon also demonstrates the reversibility of the microstructure formation.

3.2.2. Temperature-dependent oscillatory rheological studies

In order to evaluate the field-induced viscoelastic behavior of the sample, when subjected to a continuous rise in temperature and magnetic field, an oscillatory temperature ramp test is performed (Fig. 5). From this test, the variation of the G′ and G′′ moduli (Figs. 5A and B) is obtained, as a function of temperature and field, at a 0.02% strain and at a 10 Hz frequency, with a heating rate of 2 °C $\min^{-1}$. It is observed from the figures that the fluid retains strongly elastic behavior throughout the ranges of temperature (19–55 °C), i.e. G′ > G′′ in the temperature range specified for the measurement. The magnitude of G′ and G′′ at a particular field is consistent with the existing analogy that stronger field-induced structuration drives the modulus to a higher initialvalues. The effect of temperature is also obvious, i.e. a significant temperature-induced thinning is observed for all fields. However, magnitude of slopes of moduli versus temperature curves in presence of fields are much higher in magnitude than that of the zero field as aggregated structures tend to be more affected by the changes in temperature. This maybe explained in terms of higher initial field-dependent stresses. The temperature thinning effect can be attributed to number of factors, including the change in particle saturation magnetization, effect of change in carrier fluid viscosity with increasing temperature etc. Recent studies revealed that major portion of the temperature thinning effect are caused by temperature dependent behavior of the carrier fluid [21]. Effect of magnetic hysteresis and yield stress are responsible for only a slight change in moduli. It appears that all these effects are combined to produce significant temperature thinning effect for moduli under magnetic fields whereas the off-field moduli seem to be affected solely due to the changes in carrier fluid viscosity with temperature. In the tan δ (G′′/ G′) versus temperature plot (Fig. 5C), we observe no clear trend and no peaks associated to glass-transition like phenomena under the conditions specified. Provided the fact that applied strain is in LVR region, it is obvious as the sample retains strongly elastic nature (G′ > G′′) throughout the temperature window. Fig. 5D illustrates the change in complex viscosity as a function of temperature. Similar to storage modulus, complex viscosity too display temperature induced softening, i.e. viscosity decreases with increasing temperature. However, the decrease in complex viscosity without magnetic field in the temperature range of 19–55 °C is only 29% whereas a staggering 57% decrease in viscosity is reported for 0.5 T. It is obvious that the systems under magnetic fields are more strongly affected by temperature.

4. Conclusion

Fe-rich PAA-Fe_3Ni microspheres are chosen for fabrication of MR fluids for their certain features, i.e. high magnetic saturation, low coercivity and remanence and enhanced surface morphology due to polymer functionalization and capping action. The morphological studies revealed an *fcc* structure with roughly monodisperse particle distribution. The average microsphere size is 700 nm. Polymer-assisted synthesis enabled the material with soft magnetic properties and hence suitable for MR fluidic application. We have performed steady shear magnetorheology of 10 vol% MR fluid under varied magnetic fields. The yield stress scaling was also proposed for the system where, a multipolar contribution with M^3-dependence became crucial for static yield stress. The temperature-induced thinning effect was also observed in oscillatory rheology as complex moduli and viscosity both are strong functions of temperature.

Acknowledgments

One of the authors, IA thanks CSIR, India for the award of Senior Research Fellowship (SRF). The authors also thank Department of Science & Technology (DST), Govt. of India.

References

[1] G. Bossis, E. Lemaire, O. Volkova, H. Clercx, J. Rheol. 41 (687) (1997).
[2] J. Ding, G. Peng, K. Shu, C. Wang, T. Tian, W. Yang, Y. Zhang, G.G. Wallace, W. Li, Sci. Rep. 5 (2015) 15663.
[3] K. Shah, J. Oh, S. Choi, R.V. Upadhyay, J. Appl. Phys. 114 (213904) (2013).
[4] I. Arief, P.K. Mukhopadhyay, J. Magn. Magn. Mater. 412 (2016) 194–200.
[5] S.A.N. Leong, P.M. Samin, A. Idris, S.A. Mazlan, A.H.A. Rahman, Smart Mater. Struct. 25 (2016) 025025.
[6] I. Arief, P.K. Mukhopadhyay, J. Alloy. Compd. 696 (2017) 1053–1058.
[7] J.A. Ruiz-López, J.C. Fernández-Toledano, R. Hidalgo-Alvarez, J. de Vicente, Soft Matter 12 (2016) 1468–1476.
[8] A.J. Margida, K.D. Weiss, J.D. Carlson, Int. J. Mod. Phys. B 10 (3335) (1996).
[9] H. Wu, C. Qian, Y. Cao, P. Cao, W. Li, X. Zhang, X. Wei, J. Phys. Chem. Solids 71 (290) (2010).
[10] M. van Schilfgaarde, I.A. Abrikosov, B. Johansson, Nature 46 (400) (1999).
[11] R. Bolsoni, V. Drago, E. Lima Jr., J. Metastable Nanocryst. Mater. 14 (51) (2002).
[12] M. van Schilfgaarde, I.A. Abrikosov, B. Johansson, Nature 46 (400) (1999).
[13] W.H. Li, G. Chen, S.H. Yeo, H. Du, Int. J. Mod. Phys. B 16 (2002) 2725–2731.
[14] V.K. LaMer, R.H. Dinegar, J. Am. Chem. Soc. 72 (4847) (1950).
[15] P. Scherrer, Bestimmung der Grosse und der inneren Struktur von Kolloidteilchen mittels Rontgenstrahlen, Nachr. Ges. Wiss. Gottingen 26 (98) (1918).
[16] E.C. Bingham, Fluidity and plasticity, McGraw-Hill, New York, 1922.
[17] M. Ocalan, G.H. McKinley, Rheol. Acta 52 (623) (2013).
[18] D.J. Klingenberg, J.C. Ulicny, M.A. Golden, J. Rheol. 51 (883) (2007).
[19] I. Arief, P.K. Mukhopadhyay, J. Magn. Magn. Mater. 397 (57) (2016).
[20] J.M. Ginder, L.C. Davis, Appl. Phys. Lett. 65 (3410) (1994).
[21] S.G. Sherman, L.A. Powell, A.C. Becnel, N.M. Wereley, J. Appl. Phys. 117 (17C751) (2015).